SUPPLEMNTARY INFORMATION

Identifying a Li-rich superionic conductor from charge-discharge structural evolution study: Li_2MnO_3

Xiaofeng Zhang, Feng Zheng*, Shunqing Wu*, Zizhong Zhu

Department of Physics, OSED, Key Laboratory of Low Dimensional Condensed Matter Physics (Department of Education of Fujian Province), Jiujiang Research Institute, Xiamen University, Xiamen 361005, China

*E-mail: zhengfeng@stu.xmu.edu.cn (F. Zheng)

*E-mail: wsq@xmu.edu.cn (S.Q. Wu)

Supplementary Note

All possible lithium ions distribution within a supercell containing four formula units are considered. The formula of formation energy is defined as follows:

$$\Delta E_f = E_{total}(Li_xMnO_3) - \left[\frac{x}{2}E_{total}(Li_2MnO_3) + \left(1 - \frac{x}{2}\right)E_{total}(MnO_3)\right] \quad (1)$$

in which E_{total} is calculated total energy per formula unit of Li_xMnO_3 ($2 \geq x \geq 0$). The total energy of the initial state (x = 2) and the final state (x = 0) are selected as the reference points for calculating the formation energy. Furthermore, the delithiation potential is an important parameter for evaluating the performance of the cathode material, and the averaged delithiation potential associated with delithiation from the amount of x_2 to x_1 for Li_xMnO_3 ($2 \geq x \geq 0$) can be calculated by using the following expression:

$$V = -\frac{E_{total}(Li_{x_2}MnO_3) - E_{total}(Li_{x_1}MnO_3) - (x_2 - x_1)E_{total}(Li)}{(x_2 - x_1)e} \quad (2)$$

in which x_2 and x_1 are the Li composition before and after the lithium extraction from the host, respectively.

Table S1. Structural parameters of the *t*-$Li_{0.5}MnO_3$ and *t*-Li_2MnO_3.

Property	*t*-$Li_{0.5}MnO_3$	*t*-Li_2MnO_3
Crystal system	Trigonal	Trigonal
Space group	$P\bar{3}1m$	$P\bar{3}1m$
(a, b, c) (Å)	(5.048, 5.048, 4.104)	(4.928, 4.928, 5.000)
(α, β, γ) (deg)	(90.00, 90.00, 120.00)	(90.00, 90.00, 120.00)
Li1		1a (0.0000, 0.0000, 0.0000)
Li2	1b (0.0000, 0.0000, 0.5000)	1b (0.0000, 0.0000, 0.5000)
Li3		2d (0.3333, 0.6667, 0.5000)
Mn	2c (0.3333, 0.6667, 0.0000)	2c (0.3333, 0.6667, 0.0000)
O	6k (0.6439, 0.0000, 0.2472)	6k (0.3544, 0.0000, 0.7786)

Table S2. Li-ions diffusion coefficient ($D_{300\,K}$) and migration energy (E_a) for various migration pathway in *m*-Li_2MnO_3 from CI-NEB methods.

	E_a (eV)	D_{300K}(cm^2/s)
Path 1	0.68	10^{-14}
Path 2	0.69	10^{-14}
Path 3	0.70	10^{-14}
Path 4	0.54	10^{-12}
Path 5	0.65	10^{-13}

Table S3. Calculated volume and interlayer distance of *m*-Li_2MnO_3 and *t*-Li_2MnO_3.

System	Volume ($Å^3$/f.u.)	Distance (Å)
$C2/m$	52.101	4.725
$P\bar{3}1m$	52.756	4.994

Table S4. Calculated Li-ion migration distance (d), activation barriers (Ea), and estimated Li-ion diffusion coefficients (D) and ion-conductivities (σ) at room temperature.

Diffusion path	d (Å)	Ea (eV)	D (cm2/s)	σ (S/cm)
A → B	1.704	0.09	9.15 × 10-5	4.53
B → C	2.713	0.21	2.40 × 10-6	0.36
C → D	4.136	0.36	1.51 × 10-8	1.77×10-3

Table S5. Calculated phase equilibria for *t*-Li_2MnO_3. The electrochemical stability window is printed in bold.

Voltage range vs Li^+/Li (V)	Δn_{Li} per formula	Phase equilibria
0 - 1.96	4	Mn, Li_2O
1.96 - 2.44	1	$LiMnO_2$, Li_2O
2.44 - 3.62	**0**	**Li_2MnO_3**
> 3.62	-2	MnO_2, O_2

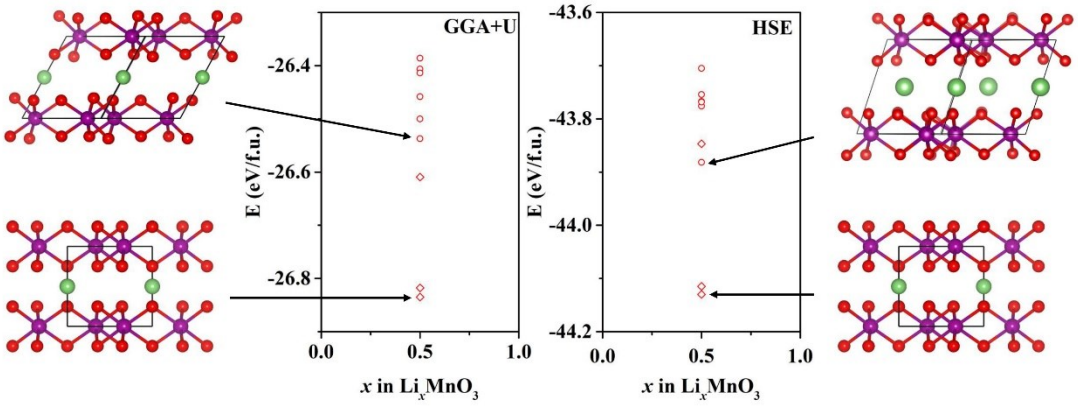

Fig. S1. The total energy calculated by the GGA+U and the single-point energy calculated by the HSE for $Li_{0.5}MnO_3$.

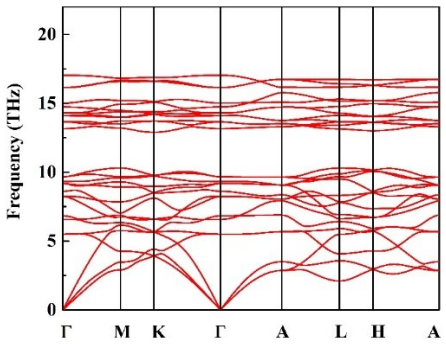

Fig. S2. Phonon band structure of *t*-$Li_{0.5}MnO_3$.

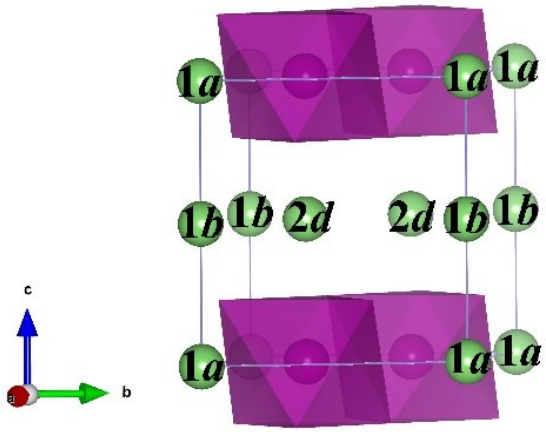

Fig. S3. Crystal structure of *t*-Li_2MnO_3.

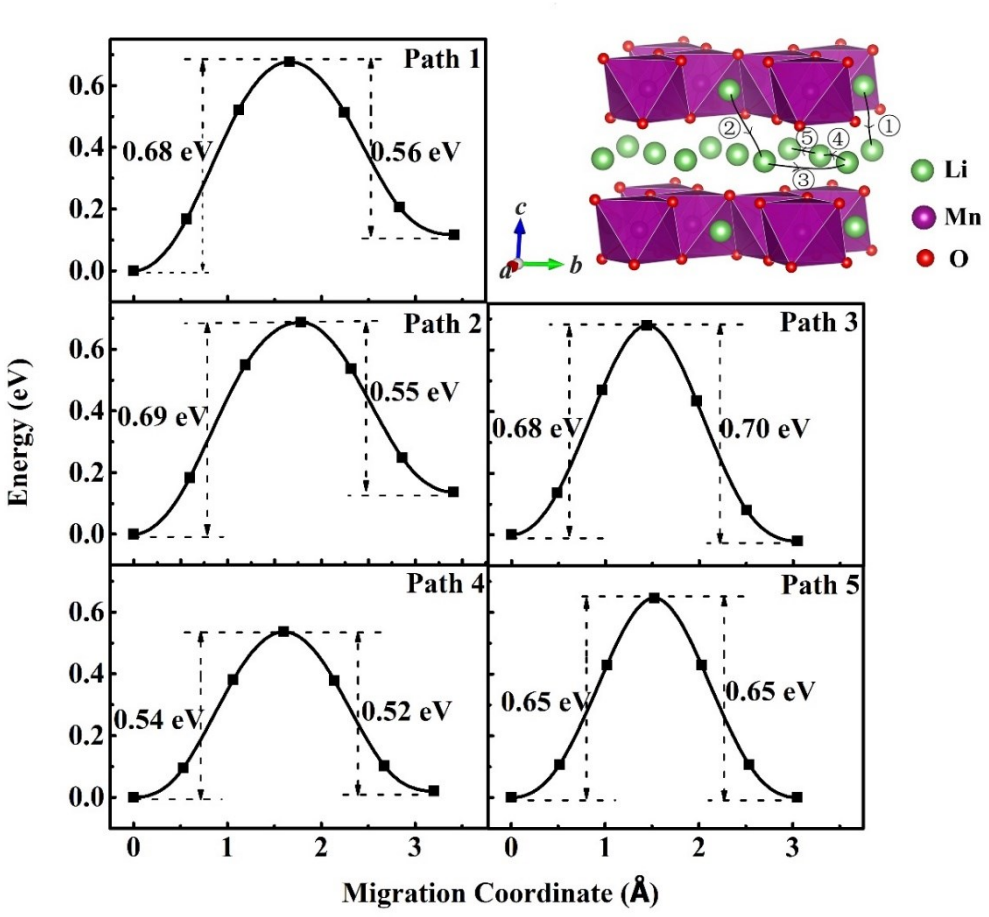

Fig. S4. Calculated kinetic properties of *m*-Li_2MnO_3. Li^+ migration channels (black arrow) and the barriers simulated by the NEB method for path 1, path 2, path3, path 4 and path 5.

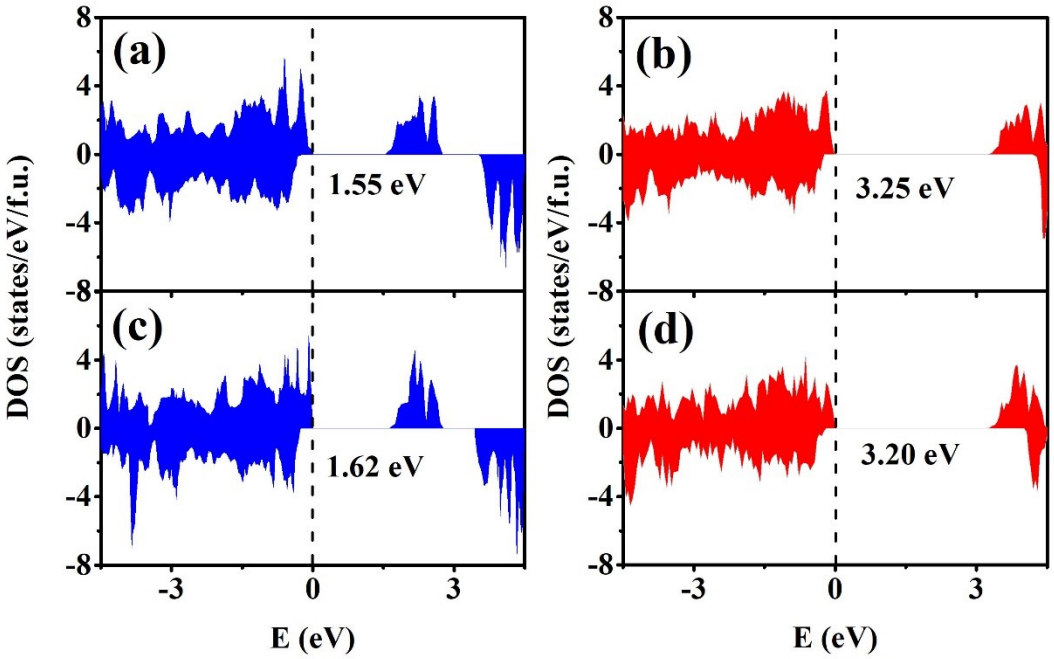

Fig. S5. The density of states (DOS) of *m*-Li_2MnO_3 calculated by (a) GGA+U and (b) HSE. The density of states (DOS) of *t*-Li_2MnO_3 calculated by (c) GGA+U and (d) HSE. The zero energy is set to the Fermi level and all energies refer to the Fermi energy. Positive and negative states represent spin-up and spin-down states, respectively.